Electrical response from nanocomposite PDMS–Ag NPs generated by *in situ* laser ablation in solution

2013 Nanotechnology 24 035707

(http://iopscience.iop.org/0957-4484/24/3/035707)

Nanotechnology **24** (2013) 035707 (9pp) doi:10.1088/0957-4484/24/3/035707

Electrical response from nanocomposite PDMS–Ag NPs generated by *in situ* laser ablation in solution

Maria Kalyva[1], Susmit Kumar[2], Rosaria Brescia[3], Simona Petroni[1], Carola La Tegola[2], Giovanni Bertoni[3,4], Massimo De Vittorio[1], Roberto Cingolani[5] and Athanassia Athanassiou[6]

[1] Center of Biomolecular Nanotechnologies @UniLe, Istituto Italiano di Tecnologia (IIT), Via Barsanti, I-73010 Arnesano, Lecce, Italy
[2] National Nanotechnology Laboratory, CNR-Istituto di Nanoscienze, Via Arnesano, 16, I-73100, Lecce, Italy
[3] Nanochemistry, Istituto Italiano di Tecnologia (IIT), Via Morego 30, I-16163 Genova, Italy
[4] IMEM-CNR, Parco Area delle Scienze 37/A, I-43124 Parma, Italy
[5] Istituto Italiano di Tecnologia (IIT), Via Morego 30, I-16163 Genova, Italy
[6] Nanophysics, Istituto Italiano di Tecnologia (IIT), Via Morego 30, I-16163 Genova, Italy

E-mail: makatrik@gmail.com (M Kalyva) and athanassia.athanassiou@iit.it

Received 3 September 2012, in final form 3 December 2012
Published 21 December 2012
Online at stacks.iop.org/Nano/24/035707

Abstract
Laser ablation technique is employed in order to generate polydimethylsiloxane (PDMS)/Ag NPs *in situ*, starting from a silver target in a solution of PDMS prepolymer and toluene. The produced surfactant-free nanoparticles are characterized by high resolution transmission electron microscopy (HRTEM) and scanning TEM-high angle annular dark field (STEM-HAADF) imaging modes, showing the majority of them to be of the order of 4 nm in diameter with a small percentage of larger Ag–AgCl multidomain NPs, embedded into a PDMS matrix. Low concentrations of carbon onion-like nanoparticles or larger fibers are also formed in the toluene–PDMS prepolymer solution. In accordance with this, UV–vis spectra shows no peak from silver NPs; their small size and their coverage by the PDMS matrix suppresses the signal of surface plasmon absorption. Inductively coupled plasma measurements reveal that the concentration of silver in the polymer is characteristically low, ∼0.001% by weight. The electrical properties of the PDMS nanocomposite films are modified, with current versus voltage (*I*–*V*) measurements showing a low current of up to a few tenths of a pA at 5 V. The surface resistivity of the films is found to be up to $\sim 10^{10}$ Ω/sq. Under pressure (e.g. stress) applied by a dynamic mechanical analyzer (DMA), the *I*–*V* measurements demonstrate the current decreasing during the elastic deformation, and increasing during the plastic deformation.

(Some figures may appear in colour only in the online journal)

1. Introduction

For the preparation of composite materials with enhanced electronic conductivity, dispersion of conductive fillers, e.g. metallic (Au, Ag, Al etc), inorganic (ZnO, ITO etc), or organic (carbon black, carbon nanotubes, conductive polymers, etc), in non-conductive polymers is proven to be an effective and low-cost method [1–3]. Extensive theoretical and experimental studies over recent decades have been focused on the electrical properties of metal–polymer composite materials due to their wide range of industrial applications such as pressure sensing elements, chemical

sensors and antistatic devices [4–6]. When nanometer size fillers are homogeneously dispersed into a polymer matrix, the composite materials are called polymer nanocomposites and have been shown to exhibit, apart from enhanced electrical properties, also unique thermal and mechanical properties [7–14].

The electrical properties of the nanocomposite films depend on different parameters, such as the size, shape, spatial distribution of nanofillers, metal content, and dielectric characteristics of the host matrix [1]. A recent study by Gornika *et al* [15] on the electrical properties of polyester and polyesterimide incorporating 100 nm silver (Ag) nanoparticles (NPs) and 10 nm silica NPs at 1.3% and 1.5% by weight concentration, respectively, has shown by using decay measurements that only nanosilver tends to improve the antistatic properties of the materials in question, although the dispersion method of the NPs is not mentioned in the work due to patent pending.

In the case of a binary composite into which spherical particles are distributed statistically, percolation theory predicts a threshold concentration of 16% by volume, where the highest performance of the properties of the composites is achieved [16, 17]. It has been shown, on the other hand, that by changing the size of the conductive fillers in the PDMS matrix from micro-sized to nano-sized, the concentration threshold necessary for an onset in conductivity is lowered [18]. Also, a decrease in the electrical resistivity of an insulating SU8 epoxy matrix, into which Ag NPs were dispersed simply by mixing, was observed for a nanofiller load of 6% vol or higher [2]. In contrast, significant changes in conductivity values are reported at extremely high content for conductive microfillers, e.g. 83 by wt% of a polydimethylsiloxane (PDMS)/Ag composite film [18], with a Ag filler size of $\sim$2 μm [2]. When the concentration of the solid conducting phase is too high, the composite becomes brittle and difficult to process as the mechanical characteristics no longer resemble those of PDMS. Especially in pressure sensing elements, where preservation of the elastic properties is a prerequisite, minimization of the concentration of the conducting phase while achieving a drop in resistivity becomes important.

Studies of the resistivity of conductive polymer composites as a function of pressure, in view of their application as pressure sensors, focus on the percolation mechanism that produces a sudden drop of resistivity at a certain value of applied pressure, making them unreliable materials for pressure sensing. Previous works have demonstrated that improvements can be obtained by designing new processing techniques in order to attain a homogeneous mix of conductive nanoparticles with the insulating polymer. In particular, wet procedures promote reproducibility of measurements and gradual resistance variation, due a better homogeneity of the nanocomposite material [19]. The preparation method of nanocomposite materials exhibiting electrical properties is very important for their ultimate response. Most of the works reporting conductive PDMS, which is the matrix used also in this work, have so far used simple mixing of the filler with the prepolymer [20, 21]. The main disadvantage of using *ex situ* processing methods is the need to use surfactants either as an intermediate step during the preparation or to facilitate uniform dispersion, even in highly diluted solutions of such a viscous medium. However, the role of surfactants in the electrical conductivity of the nanocomposite films is crucial. Nanocomposite films with nanosilver treated by five different surfactants with increasing carbon chain length and mixed into an epoxy resin showed lower electrical resistivity with decreasing surfactant chain length [22]. The PDMS elastomer is of particular interest due to its many useful properties, such as high flexibility, ease of molding, low cost, biocompatibility, and chemical inertness [23]. With recent advances in soft lithography and polymer microelectromechanical systems (MEMSs), PDMS can be incorporated into a large range of micrometer and nanometer scale devices for many different applications, e.g. biological and medical applications, microelectronics, etc [24]. Moreover, Ag is the metallic filler of choice in this work, as it has the highest electrical conductivity compared to other nanostructured metal particles [25].

To the best of our knowledge, the preparation methods for producing NPs *in situ* in PDMS involve the reduction of a precursor into the prepolymer, the simultaneous reduction of Ag precursor by radical polymerization of monomers or the thermal evaporation of different metals, e.g. Au, Ag, Fe into the prepolymer [26, 27]. In the above mentioned methodologies limitations arise as it is difficult to control the reduction of the precursor and, therefore, to produce monodispersed distributions of NPs in the matrix. The latter methodology produces better distributions of the Ag NPs in the films, but in order to incorporate them into the whole depth of the matrix, a lot of thermal treatments are required, resulting in continuously affecting the matrix. Herein, we present for the first time a one step method for producing surfactant-free Ag NPs *in situ* in a toluene solution of PDMS prepolymer by laser ablation (LA). The majority of the produced NPs are of the order of 4 nm in diameter, while a small percentage of larger Ag–AgCl multidomain NPs exist inside the PDMS matrix. By increasing the laser irradiation time we produced Ag NPs in toluene/prepolymer solutions with increasing but still characteristically low concentrations. Although the concentration of NPs in the PDMS/Ag nanocomposite was low, we were able to acquire the onset of current in the *I–V* characteristics. Also, we were able to probe small variations in the current response of the composite material caused by miniscule alterations in the concentration of the Ag NPs. Finally, a pressure sensitive response was detected in PDMS/Ag composites fabricated using our reported *in situ* laser ablation method for Ag NPs.

2. Methods

2.1. Ag NP formation by LA and film preparation

Silver NPs were prepared by LA of a Ag metal rod (diameter 9 mm $\times$ thickness 6 mm, >99.99% purity) in a highly diluted solution of PDMS prepolymer. Different solvents were tested such as toluene, hexane, ethanol, methanol, and chloroform.

The most transparent and adequately diluted solution was PDMS prepolymer and toluene, resulting to be the most suitable for LA. The metal rod was placed on the bottom of a glass cuvette filled with 1.5 ml of the solution in all experiments. The rod was irradiated with the second harmonic (532 nm) of a Nd:YAG laser (Quanta-Ray GCR-190, Spectra Physics) operating at 10 Hz and with a pulse duration of <7 ns on a rotating base with a speed of 4.5° s^{-1}. The laser pulse energy was 4.6 mJ/pulse, the spot diameter was measured to be 0.3 mm and, therefore, the fluence was roughly estimated to be 6.5 mJ cm^{-2}. In all measurements the laser beam was focused by a lens ∼1 mm below the surface target and the irradiation time was varied from 0.5 to 3.0 h. Every 0.5 h, 0.1 μl of toluene was refilled to recover the initial liquid level due to evaporation during irradiation in order to avoid any agglomeration of the NPs. Upon irradiation, the solution gradually turned light yellow in color in all cases. After the evaporation of the toluene during stirring, the viscous solution remained over night in a dessicator. After addition of the cross-linker in 10:1 ratio, the resulting composite was drop cast onto the devices and baked at 140 °C for 10 min.

2.2. UV–vis spectrophotometer

The absorption spectra of the colloidal solutions were acquired immediately after the end of the irradiation time by a Cary UV–visible spectrophotometer.

2.3. TEM sample preparation and analysis

TEM analyses were carried out on the NPs both dispersed in the liquid PDMS prepolymer–toluene solution and embedded in the solidified films. For the first type of sample, one drop (∼100 μl) of the dispersion was deposited onto a copper grid covered with an ultrathin amorphous carbon film. For the second type of sample, electron-thin samples were obtained by means of cryo-ultramicrotomy. Thin slices (∼70 nm thick) were cut from the hardened sample at low temperature (∼−160 °C) using a Leica EM FC6 ultramicrotome. These thin slices were then placed onto a standard carbon-coated copper grid. The TEM analyses were performed using a JEOL JEM-2200FS microscope operated at 200 kV equipped with a CEOS aberration corrector in the objective lens, with an information limit of 1.1 Å [28]. The microscope had a scanning STEM unit (Gatan Digiscan II) with an HAADF detector, with a point resolution of 1.9 Å in STEM-HAADF mode. Energy dispersive spectrometry (EDS) x-ray spectra were acquired using a Si(Li) detector (JEOL JED-2300) from selected areas of the HAADF images with continuous drift correction. High resolution TEM (HRTEM) analyses were carried out on the NPs formed in the liquid solution.

2.4. Inductively coupled plasma (ICP) technique

Inductively coupled plasma (ICP) technique was employed in order to quantify the metallic phase in the prepared colloidal solutions. The samples were transferred into ICP flasks, dried with acetone and digested with 1 ml of aqua regia. After 24 h the samples were diluted up to 10 ml with filtered milli*Q* water. The diluted solutions were then filtered on syringe filters (0.22 μm) and analyzed by ICP. Ag peaks were detected from the solution at three different wavelengths, in accordance with standard silver solutions, which are associated with the Ag concentration. After 3 h of laser ablation of the Ag target in solution of prepolymer in toluene, the measured concentration was ∼0.046 377 ppm, which is close to the limit of the equipment. Knowing the grams and density of the PDMS prepolymer, we calculated the percentage by weight concentration of Ag in the polymer to be of the order of 0.001%.

2.5. I–V measurements and surface resistivity calculations

Conductivity measurements took place either on films drop cast onto devices (Au electrodes evaporated onto SiO_2(500 nm)/Si), or directly on glass substrates. 350 nm length Au electrodes were separated by a 250 nm gap, having a thickness of 100 nm. These samples were measured in ambient conditions on a Karl Suss 4-probe probe station. A parameter analyzer was used to apply the required bias voltage. Before deposition of the Ag–PDMS film, the devices were measured to assess the quality of the open contacts (∼fA at 5 V). The surface resistivity, which is defined as the resistance to leakage current along the surface of an insulating material and is a characteristic property of the material, was also measured for these samples. The surface resistivity was calculated taking into consideration its definition which is the quotient of the potential gradient, in V m^{-1}, and the current per unit of electrode length, in A m^{-1}, ASTM Standard D 257-99 [29].

2.6. Profilometer measurements

The thicknesses of the PDMS nanocomposite films that were drop cast onto the devices (Au electrodes evaporated onto SiO_2(500 nm)/Si) were measured in the center of the device by cutting the layer and scanning the step, the height of which was found to be about 10.2 μm. The measurement was performed using a KLA Tenkor P-11 long scan profiler by applying a minimum force of 1 mg on the stylus in contact with the soft sample.

2.7. Dynamic mechanical analyzer (DMA)

The ability of the material to be deformed under the influence of pre-fixed stresses (creep) was investigated using a Q800 DMA from TA instruments. In this way, when the load is kept uniform for a fixed time, the deformation of the material is stable even when the material is loaded with stresses under the yield strength value. Stressing the material in this way gives the opportunity to observe the electrical effects before, during, and after the load is applied. For this purpose, an electrically isolated pressure clamp was used with a matching round head of 0.85 mm in diameter. A preload force of 0.001 N guaranteed constant contact between the pressure head and the specimen. The creep time and recovery time were fixed equal

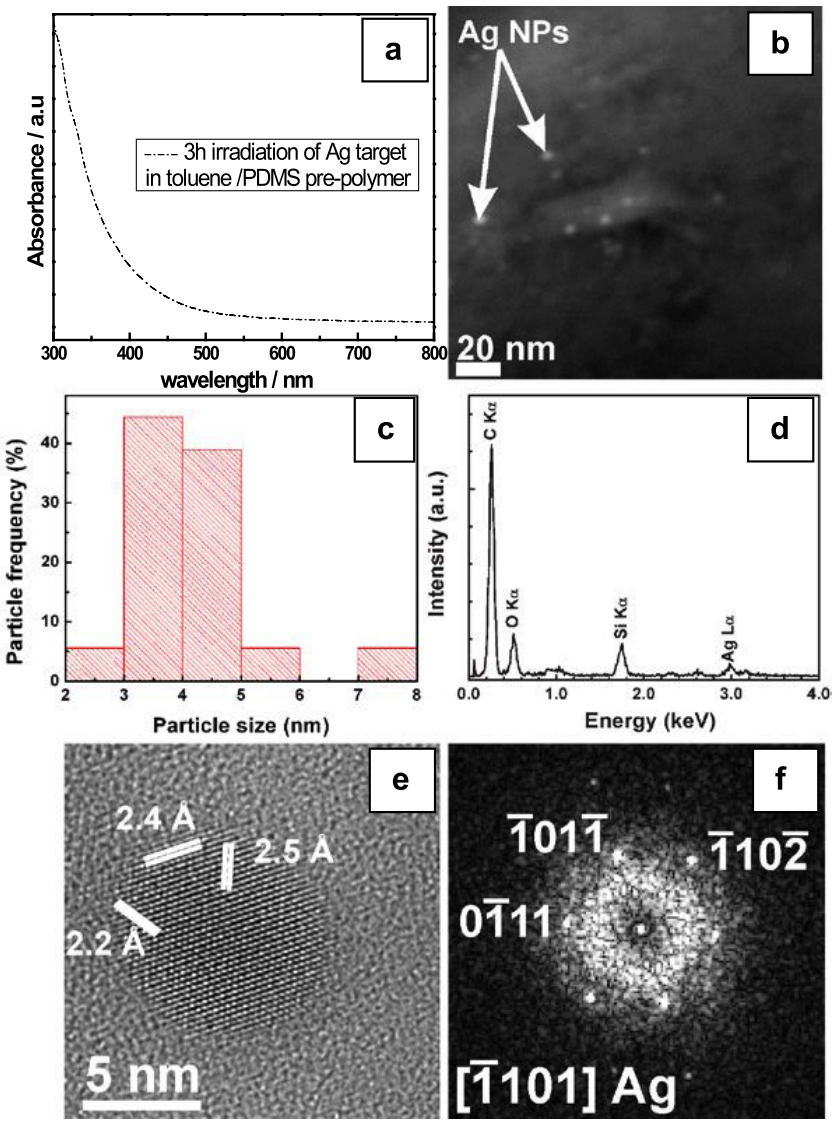

Figure 1. (a) The UV–vis spectrum of Ag NPs obtained after 3 h of irradiation by laser ablation in toluene and PDMS prepolymer solution. (b) STEM-HAADF of Ag NPs inside the PDMS matrix. (c) The size distribution of the majority of the produced NPs, with an average size of 4.2 (±0.9) nm. (d) The EDS spectrum acquired from an area including several NPs, showing the characteristic peaks for Ag, due to the NPs, together with O, C, and Si, generated by the matrix and the carbon support film. (e) An HRTEM image and (f) the corresponding FT of one of the larger NPs (∼9 nm), showing a single crystal structure ascribable to hexagonal Ag ($a = b = 2.886$ Å, $c = 10.0$ Å, PDF #411402).

to 6 min for all the five applied stresses (0.1, 0.5, 1.0, 5.0 and 10.0 MPa) in ambient conditions. The apparatus responded to the standard ASTM D 2990-01 (Standard Test Methods for Tensile, Compressive and Flexural Creep and Creep-Rupture of Plastics).

3. Results and discussion

3.1. Preparation and characterization of the Ag NPs in the PDMS prepolymer and toluene solution

Laser ablation of solid targets into liquids is a recent alternative physical method for fabrication of NPs [30, 31]. One of the main advantages is that the generated NPs are surfactant free, which is not the case for other techniques, e.g. chemical synthesis, electrochemical deposition, etc [32]. In particular, LA in water is a rather simple and rapid technique and it allows control of the NP size and size distribution by variation of parameters, e.g. laser fluence, irradiation time, focusing of the laser to the target surface, etc [33]. Laser ablation in organic solvents has also been studied for controlling the size, but also for direct functionalization of the generated NPs [30]. There have been several attempts to control the particle size and size distribution, or improve the particle stability, by adding surfactants, organic solvents, polymers, and thiolated ligands to the solution [34, 35]. Generally, a trend was observed when comparing the size of noble metal NPs obtained in water and in organic solvents, with the size of the NPs obtained in water resulting to be larger than the size produced in organic solvents [36].

We employed the second harmonic of a Nd:YAG laser at 532 nm. The silver target was immersed in a PDMS prepolymer and toluene solution, and irradiated for different times of up to 3 h. PDMS is well known to swell extensively in non-polar solvents such as toluene, and therefore a highly diluted and transparent solution is formed when it is mixed with the prepolymer [22, 37]. Highly diluted and transparent solutions, e.g. prepolymer and toluene, are appropriate for the laser pulses to reach the target surface. After LA, our solutions were characterized by UV–vis spectroscopy, showing no plasmon peak (figure 1(a)). Amendola *et al* [38] demonstrated similar quenching of the UV–vis plasmon resonance peak corresponding to Au NPs produced in toluene by laser ablation. They attributed the quenching of the plasmon resonance to the strong interaction of organic solvents with the surface of NPs. They reported an extremely small size of the NPs embedded within a graphitic matrix.

As is already known, LA in non-aqueous liquids causes their thermal decomposition down to elementary carbon, while there are several works reporting the production of carbon glass nanoparticles [39, 40]. We performed micro-Raman measurements in random points of the nanocomposite films finding no evidence of glass carbon (not shown here). However, this can be explained since, as stated in these works, the essential feature of the process is the high repetition rate of laser pulses of 10 kHz, which favors the accumulation of carbon species in the medium, in contrast to our case of low laser repetition [41]. Also, carbon particle production was mainly reported in the environment of a solvent, such as ethanol, toluene, benzene etc, while we have a more complex environment of toluene/PDMS prepolymer that may not favor or may even hinder their production.

In our case, the Ag NPs produced in the PDMS prepolymer/toluene appear to be embedded in a matrix, as seen by STEM-HAADF at medium resolution, with the contrast indicating different mean atomic numbers (figure 1(b)). The size distribution of the majority of the Ag NPs is around 4 nm, as can be seen from the histogram (figure 1(c)). In order to assess the nature of the matrix surrounding the NPs, we acquired EDS spectra from areas including several NPs. Characteristic peaks of Ag, originating from the Ag NPs, as well as O, C and Si peaks generated by the matrix, were observed in figure 1(d). In figure 1(e) an HRTEM image of a relatively large (∼9 nm) NP is presented, and in figure 1(f) its corresponding Fourier transform, showing a single crystal structure ascribable to hexagonal Ag. The smaller NPs show instead multiple twinning in HRTEM (not shown here), with mostly cubic Ag structure.

Apart from small Ag NPs, Ag–AgCl multidomain NPs were detected inside the PDMS matrix, as seen in STEM-HAADF (figure 2(a)). From a rough estimation of the acquired images, the ratio of small NPs to multidomains is 10:1 or even higher, meaning that the small NPs are prevalent. In figure 2(b) an HRTEM image from a Ag–AgCl multidomain inside the PDMS matrix is shown. The patterns inside the brighter and the darker regions fit to cubic AgCl and cubic Ag, respectively. The size of the Ag NPs participating in multidomains is larger (9 ± 3 nm) compared to the majority of Ag NPs. Their larger size is due to some kind of agglomeration due to solvent evaporation either during laser ablation or during film preparation that cannot be avoided. Figure 2(c) shows an EDS spectrum acquired from a AgCl particle in a Ag–AgCl multidomain inside the PDMS matrix. The Ag/Cl atomic ratio, evaluated for several particles, is

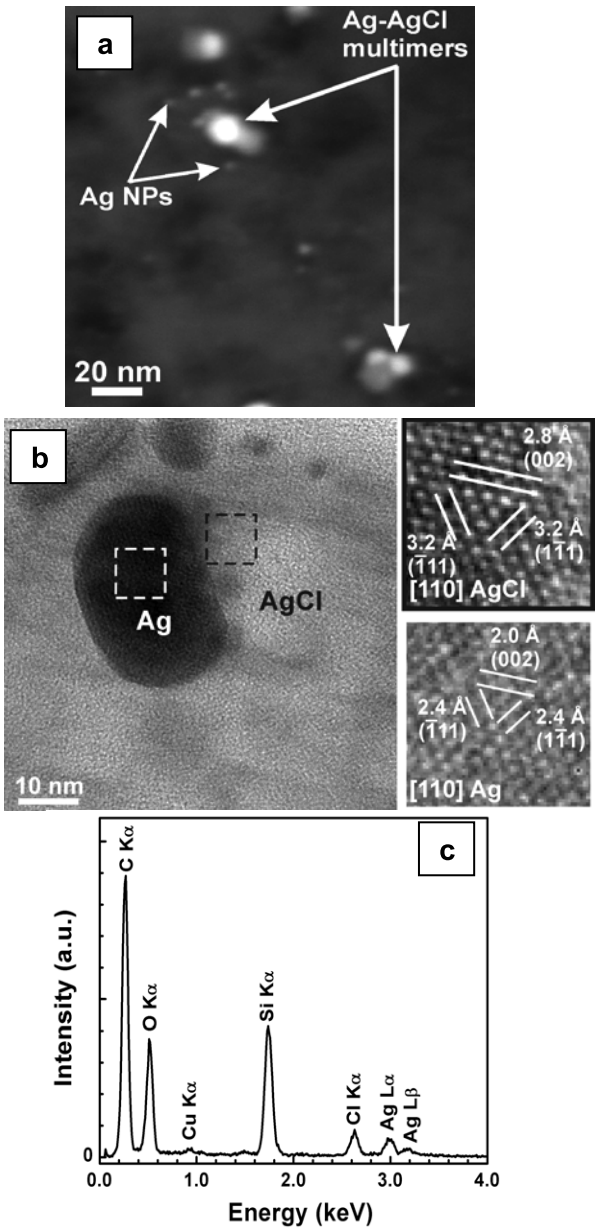

Figure 2. (a) An STEM-HAADF image of small (4.2 (±0.9) nm) Ag NPs and Ag–AgCl multidomains (with the Ag NPs in multidomains being 9 (±3) nm). (b) Left: an HRTEM image of a region with a large Ag–AgCl multidomain inside the PDMS matrix. The patterns inside the brighter region (top right) and the darker region (bottom right) fit to cubic AgCl ($a = 5.5491$ Å, PDF #311238) and cubic Ag ($a = 4.0862$ Å, PDF #040783), respectively. (c) An EDS spectrum acquired from a AgCl particle in a Ag–AgCl multidomain inside the PDMS matrix. The Ag/Cl atomic ratio, evaluated for several particles, is 1.0 (±0.2). The signals from Si, C and O are due to the PDMS polymer matrix and the carbon support film.

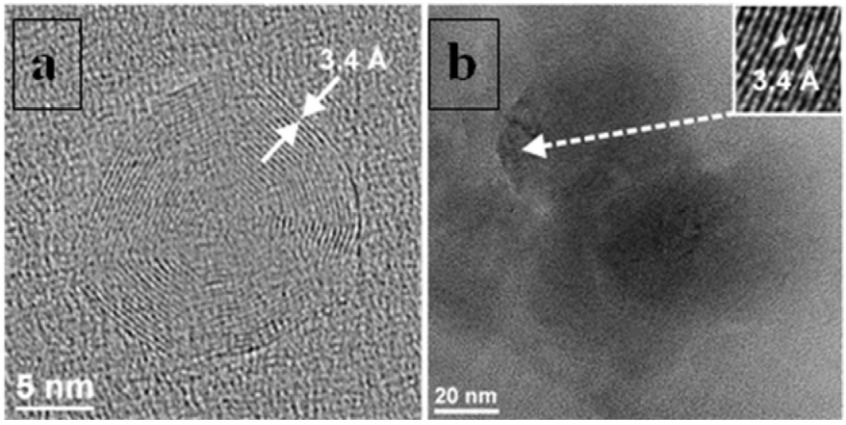

Figure 3. HRTEM images of (a) an onion-like nanoparticle and (b) a larger carbon fiber, representative of the partial graphitic structures rarely found in the samples obtained by *in situ* laser ablation of a Ag target in PDMS prepolymer and toluene solution. The spacing between adjacent planes corresponds to the typical spacing between graphite basal planes.

1.0 ± 0.2. The signals from Si, C and O are due to the PDMS polymer matrix and to the carbon support film.

The presence of Cl is attributed to a small amount of contamination that we could not control or to the prepolymer itself since two of the three steps of silicone synthesis involve the presence of chlorosilane compounds [42]. In any case, the observed negligible amounts of chlorine present as AgCl in the sample do not appear to influence the conduction properties and, as was already reported previously, AgCl NPs do not hinder the conduction of polymer composite films [43].

Finally, a very small number of carbon onion-like nanoparticles or larger fibers were detected inside the PDMS matrix, as seen in the HRTEM images (figures 3(a), (b)). They represent partial graphitic structures rarely found in the samples, with the spacing between adjacent planes corresponding to the typical spacing between graphite basal planes. The formation of the carbon onion-like nanoparticles is possible through a mechanism that was reported to be attributed to the catalytic effect of silver that lowers the temperature for the carbon graphitization and the increased mobility of carbon atoms at high temperature favoring this particular structure [44]. These carbon onion-like structures have been reported to exhibit electrical conductivity [45]. We believe that, as we have already mentioned that the electrical conductivity of silver is the highest, the presence of these very few carbon species may assist with a small contribution to the conductivity of the nanocomposite films.

ICP measurements demonstrated that the concentration of the metallic to the organic phase was characteristically low. After 3 h of laser ablation of the Ag target in the solution of prepolymer and toluene the measured concentration of ∼0.046 377 ppm (calculated to be of the order of 0.001 wt%) was close to the limit of the measurement capability of the equipment.

Considering that under the same laser ablation conditions the irradiation time should not significantly affect the etching rate, we estimated the Ag concentration in the solution for shorter irradiation durations. Therefore, by using laser ablation we introduced surfactant-free NPs *in situ* into the PDMS prepolymer with most of them being small, ∼4 nm in diameter, a small percentage of larger Ag–AgCl NPs and a very small number of carbon onion-like nanoparticles and larger fibers. The introduction of Ag NPs by this method into the nanocomposite films even at low Ag by wt% concentrations allows the measurement of conduction characteristics.

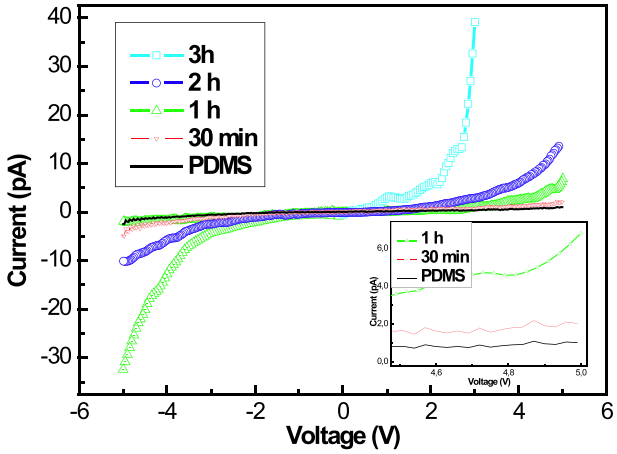

Figure 4. The *I*–*V* response of PDMS–Ag nanocomposite films drop cast onto devices (Au on SiO_2(500 nm)/Si). The curves show the variation in current versus voltage for films prepared after 0 min (black), 30 min (red), 1 h (green), 2 h (blue), and 3 h (cyan) of laser ablation of a Ag target into a toluene and PDMS prepolymer solution, respectively.

3.2. DC electrical characteristics

Conductivity measurements were carried out for different Ag concentrations after different irradiation times of 30 min, 1, 2, and 3 h (figure 4), with the conductivity of net PDMS presented for comparison. The nanocomposite polymeric films were prepared by drop casting onto Au electrodes evaporated onto SiO_2(500 nm)/Si (all electrodes were checked for electrical shorts) and were baked at 140 °C.

After 1 h of laser ablation a very low conductivity of the order of a few pA was detected at 5 V applied

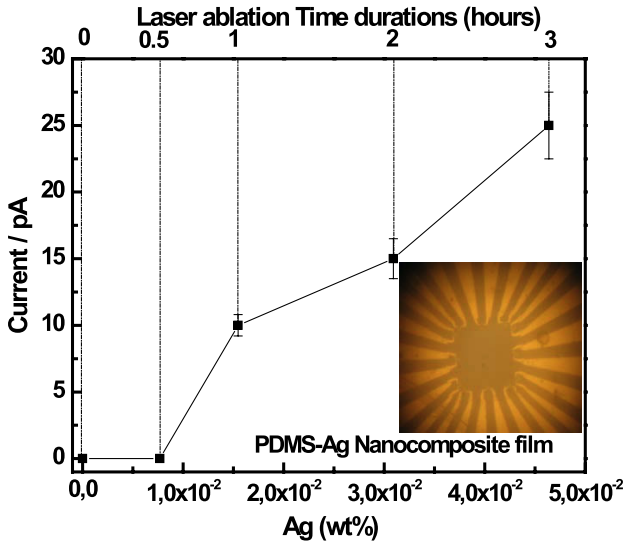

Figure 5. Current values at 5 V applied bias with statistical errors as a function of Ag concentration in the PDMS films, corresponding to different laser ablation times. Inset: microscope image of a PDMS/Ag film after 3 h of irradiation, deposited on the device (Au electrodes evaporated onto SiO_2(500 nm)/Si).

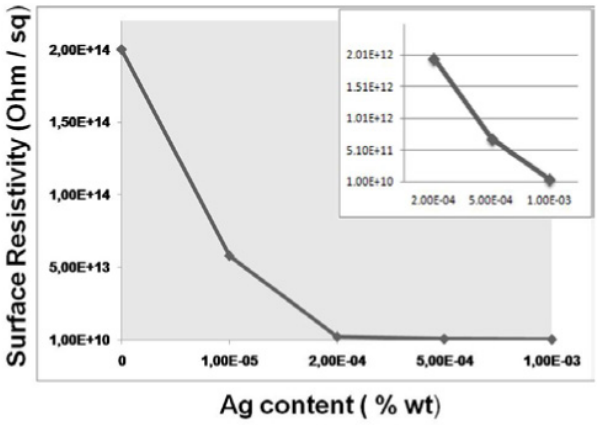

Figure 6. The surface resistivity of PDMS/Ag nanocomposites varies from 10^{10} to 10^{13} Ω/sq (at 3 V) by increasing the Ag content. Inset: magnification of the trend for values of Ag content ranging from 10^{-3} to 10^{-4} (wt%).

bias. Increasing the Ag concentration by increasing the irradiation time into the PDMS, we observed an increase in the value of the output current, as shown in figure 5, for 5 V applied bias. Since by changing the irradiation time we are still in the same low silver concentration range scale, a large change in *I–V* response would be rather unexpected. As stated above, the quantity of NPs produced by laser ablation is rather low, which is considered a drawback of the technique [38]. *I–V* measurements were performed on five different devices for each Ag concentration produced by varying the irradiation duration. In order to be certain of the detected current values and general current trend, a number of repetitions of the measurements for each Ag concentration in the PDMS film were performed, leading to the occurrence of a statistical error in the measurements (figure 5). A microscope image of a PDMS/Ag film after 3 h of irradiation deposited on the device is also shown. Taking into account the existing charge transport mechanisms previously mentioned in the literature to explain the conductivity of such nanocomposites, tunneling-type transport is unlikely considering the low quantity of Ag fillers. The transport mechanism at room temperature in such an insulating medium is expected to be a combination of activated-type and hopping-type processes [46]. Due to the fact that the *I–V* measurements of our films were conducted on devices of known electrode and area dimensions, using the measured values it was possible to deduce the surface resistivity (ρ_s) of our materials from the equation

$$\rho_s = (VD)/(I_s L), \tag{1}$$

where V is the applied bias voltage, D is the width of the film, I_s is the surface current, and L is the distance between the electrodes [29]. The surface resistivity values of our nanocomposites varied from 10^{10} to 10^{13} Ω/sq at 3 V, as seen in figure 6. For the PDMS film without the introduction of Ag NPs, the surface resistivity was found to be above 10^{14} Ω/sq. Thus, by adding surfactant-free small Ag NPs generated *in situ* into the PDMS prepolymer, we have succeeded in decreasing by three to four orders of magnitude the surface resistivity of the polymer film. Generally, for a material to be addressed as antistatic, the surface resistivity values must range from 10^9 to 10^{14} Ω/sq [47]. Therefore, we managed to produce an antistatic material from an insulating one by adding miniscule amounts of Ag.

3.3. I–V characteristics versus pressure

In order to observe the *I–V* characteristics as a function of applied pressure, a nanocomposite polymeric film was produced by drop casting the solution prepared after 3 h of irradiation of the Ag target in PDMS prepolymer/toluene onto a metal layer of molybdenum (Mo) (150 nm thick) previously deposited by sputtering. On this PDMS–Ag nanocomposite film a top electrode of Mo was deposited using a shadow mask. *I–V* measurements were performed under different pressures of 0.1, 0.5, 1.0, 5.0, and 10.0 MPa applied by a dynamic mechanical analyzer (DMA) in compression mode. The current was generated between the two parallel plate electrodes by applying a step bias voltage of up to 10 V. It is important to note that for net PDMS film, no current was detected after applied pressure. We observed current values of the order of few tens of pA, as shown in figure 7(a). Up to 1 MPa of applied stress the current across the nanocomposite film was gradually reduced, a result demonstrating the potential of the system as a pressure sensor. From 5 MPa onwards the current started to increase, as can be seen in figure 7(b).

Generally, the mechanical properties of PDMS vary with preparation conditions, but literature values for the Young's modulus are around 2 MPa [48, 49]. The mechanical strain recorded with time demonstrates that at approximately ∼5 MPa plastic deformation of the film starts to occur

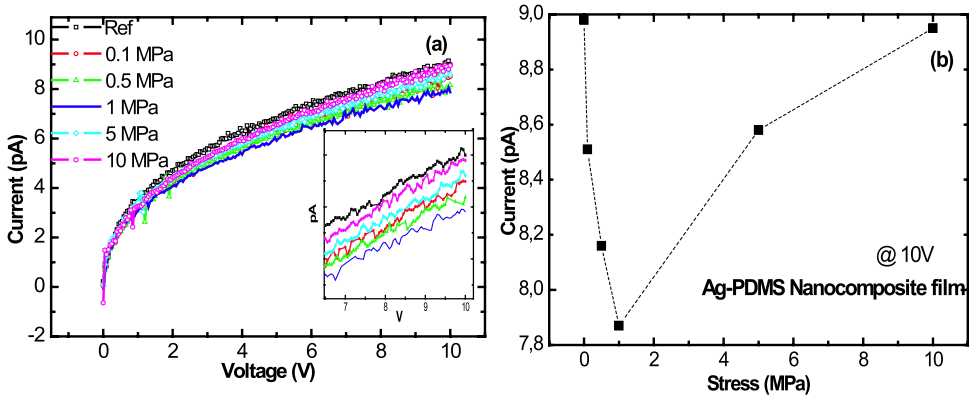

Figure 7. (a) Current values for a PDMS/Ag nanocomposite film by applying a step bias voltage of up to 10 V between two parallel plate Mo electrodes. A decrease in conductivity before plastic deformation and an increase after plastic deformation were observed by increasing the stress applied by the DMA. (b) Current values at 10 V as a function of applied stress on a PDMS/Ag nanocomposite film, showing the initial drop and subsequent increase in conduction.

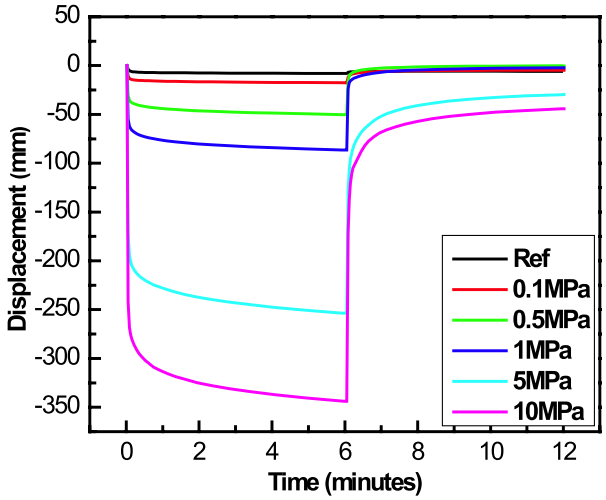

Figure 8. Displacement recorded as a function of time for PDMS/Ag nanocomposite films at increasing values of stress, showing plastic deformation above 5 MPa.

(figure 8), since the recovery of the sample's displacement is not complete after removal of the applied stress. As reported by Ruschau *et al* [45], this deformation is necessary to reduce the constriction resistance and guarantee a good electrical contact, which is confirmed by the *I–V* measurements, whereas the current decreases with the applied pressure as long as the deformation is elastic. Once plastic deformation occurs the current starts to increase, i.e., additional conductive pathways are created within the composite even at a very low concentration of Ag NPs incorporated in the PDMS. Therefore, the developed system can be used also as indicator for the occurrence of plastic deformation in nanocomposite materials.

4. Conclusions

A novel method is proposed for the preparation of nanocomposite Ag/PDMS films which exhibit interesting electrical properties. Surfactant-free Ag NPs were fabricated *in situ* by laser ablation of a silver target into a PDMS prepolymer and toluene solution. During laser ablation we generated small Ag NPs about 4 nm in diameter, a small percentage of larger Ag–AgCl multidomain NPs, and a very small number of carbon onion-like nanoparticles and larger fibers. By increasing the laser irradiation time we increased the generation of the Ag NPs and the carbon species, which was revealed by the increase in the current response in the *I–V* characteristics. Since these carbon species are rarely seen in the films, we believe that they may assist with a small contribution to the conductivity but not to be as crucial as the Ag NPs. Therefore, we were able to tune the surface resistivity of these nanocomposite materials even at minimum Ag concentrations. By measuring the output current we observed a highly sensitive response of bulk Ag/PDMS films as a function of the applied pressure. Their high sensitivity in current response, obtained either by changing the irradiation time (and therefore the Ag concentration) or by applying pressure, while preserving the elastic nature of the polymer, renders them suitable materials for applications as antistatic coatings, pressure sensors, and chemical sensors.

Acknowledgments

The authors would like to thank Alberto Ansaldo for Raman measurements. RB and GB gratefully acknowledge Roberta Ruffilli for TEM sample preparation.

References

[1] Zois H, Apekis L, Yevgen P and Mamunya Y P J 2003 *Appl. Polym. Sci.* **88** 3013
[2] Jiguet S, Bertson A, Hofmann H and Renaud P 2005 *Adv. Funct. Mater.* **15** 1511
[3] Wouters M E L, Wolfs D P, Van der Linde M C, Hovens J H P and Tinnemans A H A 2004 *Prog. Org. Coat.* **51** 312
[4] Bhattacharya S K 1986 *Metal-Filled Polymers: Properties and Applications* (New York: Dekker)
[5] Norman R H 1970 *Conductive Rubbers and Plastics* (NewYork: Elsevier)

[6] Delmonte J 1990 *Metal/Polymer Composites* (New York: Van Nostrant-Reinhold)
[7] Kozako M, Yamano S, Kido R, Ohki Y, Kohtoh M, Okabe S and Tanaka T 2005 *Proc. Int. Symp. on Electrical Insulating Materials* vol 1 p 231
[8] Tanaka T 2005 *IEEE Trans. Dielectr. Electr. Insul.* **12** 914
[9] Zou C, Fothergill J C, Fu M and Nelson J K 2006 Improving the dielectric properties of polymers by incorporating nano-particles *Proc. 10th Int. Conf. on Electrical Insulation (INSUCON) (Birmingham, May)*
[10] Lai Y H, Kuo M C, Huang J C and Chen M 2007 *Mater. Sci. Eng.* A **158** 458
[11] Li H, Liu G, Liu B, Chen W and Chen S 2007 *Mater. Lett.* **61** 1507
[12] Cheng L, Zheng L, Li G, Zeng J and Yin Q 2008 *Physica* B **403** 2584
[13] Pavlidou S and Papaspyrides C D 2008 *Prog. Polym. Sci.* **33** 1119
[14] Aso O, Eguiaza'bal J I and Naza'bal J 2007 *Compos. Sci. Technol.* **67** 2854
[15] Gornika B, Mazur M, Sieradzka K, Prociow E and Lapinski M 2010 *Acta Phys. Pol.* A **117** 869
[16] Kirkpatrick S 1973 *Rev. Mod. Phys.* **45** 574
[17] Zallen R 1983 *The Physics of Amorphous Solids* (New York: Wiley)
[18] Niu X, Peng S, Liu L, Wen W and Sheng P 2007 *Adv. Mater.* **19** 2682
[19] Hussain M, Choa Y H and Niihara K 2001 *J. Mater. Sci. Lett.* **20** 525
[20] Niu X Z, Wen W J and Lee Y K 2005 *Appl. Phys. Lett.* **87** 243
[21] Park J H, Lim Y T, Park O O, Kim J K, Yu J W and Kim Y C 2004 *Chem. Mater.* **16** 688
[22] Jiang H, Moon H K S, Lu J and Wong C P 2005 *J. Electron. Mater.* **34** 1432–9
[23] Lee J N, Park C and Whitesides G M 2003 *Anal. Chem.* **75** 6544
[24] Abbasi F, Mirzadeh H and Katbab A A 2001 *Polym. Int.* **50** 1279
[25] Chang L T and Yen C C 1995 *J. Appl. Polym. Sci.* **55** 371
[26] Kim J Y, Shin D H, Ihn K J and Suh K D 2003 *J. Indust. Eng. Chem.* **9** 37
[27] Salz D, Wark M, Baalmann A, Simonc U and Jaeger N 2002 *Phys. Chem. Chem. Phys.* **4** 2438
[28] Bertoni G, Grillo V, Brescia R, Ke X, Bals S, Catellani A, Li A H and Manna L 2012 *ACS Nano* **6** 6453–61
[29] Maryniak W A, Uehara T and Noras M A 2003 *Trek Inc. Appl. Note* **1005** 1
[30] Mafune' F, Kohno J, Takeda Y and Kondow T 2001 *J. Phys. Chem.* B **105** 9050
[31] Sibbald M S, Chumanov G and Cotton T M 1996 *J. Phys. Chem.* **100** 4672
[32] Besner S, Kabashin A V and Meunier M 2006 *Appl. Phys. Lett.* **89** 233122
[33] Kalyva M, Bertoni G, Milionis A, Cingolani R and Athanassiou A 2010 *Microsc. Res. Tech.* **73** 937
[34] Compagnini G, Scalisi A A and Puglisi O 2002 *Phys. Chem. Chem. Phys.* **4** 2787
[35] Kabashin A V and Meunier M 2006 *J. Photochem. Photobiol.* A *Chem.* **182** 330
[36] Amendola V and Meneghetti M 2009 *Phys. Chem. Chem. Phys.* **11** 3805
[37] Gevers L E M, Vankelecom I F J and Jacobs P A J 2006 *J. Membr. Sci.* **278** 199
[38] Amendola V, Rizzi G A, Polizzi S and Meneghetti M 2005 *J. Phys. Chem.* B **109** 23125
[39] Kuzmin P G, Shafeev G A, Bukin V V, Garnov S V, Farcau C, Carles R, Warot-Fontrose B, Guieu V and Viau G 2010 *J. Phys. Chem.* C **114** 15266
[40] Kazakevich P V, Simakin A V, Voronov V V and Shafeev G A 2006 *Appl. Surf. Sci.* **252** 4373
[41] Simakin A V, Obraztsova E D and Shafeev G A 2000 *Chem. Phys. Lett.* **332** 231
[42] Dow Corning Corporation 1997 *Midland Michighan USA 48686-0994, Form No.* 51-9604-97 Silicone Cheminstry Overview
[43] Pinte'r E, Patakfalvi R, Fulei T, Gingl Z, Dekany I and Visy C 2005 *J. Phys. Chem.* B **109** 17474
[44] Cabioc'h Th, Thune E and Jaouen M 2002 *Phys. Rev.* B **65** 132103
[45] Kuznetsov V L, Butenko Yu V, Chuvilin A L, Romanenko A I and Okotrub A V 2001 *Chem. Phys. Lett.* **336** 397
[46] Shih W P, Tsao L C, Lee C W, Cheng M Y, Chang C, Yang Y J and Fan K C 2010 *Sensors* **10** 3597 www.ece.rochester.edu/∼jones/demos/definitions.html (Up to 8/12/2011)
[47] Bietsch A and Michel J 2000 *J. Appl. Phys.* **88** 4310
[48] Stafford C M, Guo S, Harrison C and Chiang M Y M 2005 *Rev. Sci. Instrum.* **76** 062207
[49] Ruschau G, Yoshikawa S and Newnham R E 1992 *J. Appl. Phys.* **22** 953